




Dendritic cell-targeting chemokines inhibit colorectal cancer progression

Pengkun Yuan^{1,2,3}, Yunyi Zhou^{1,2}, Zhixue Wang^{1,2}, Liming Gui^{1,2}, Bin Ma^{1,2*} 

¹School of Biomedical Engineering, Med-X Research Institute, Shanghai Jiao Tong University, Shanghai 200030, China

²Clinical Stem Cell Research Center, Renji Hospital, School of Medicine, Shanghai Jiao Tong University, Shanghai 200127, China

³Zhejiang University–University of Edinburgh (ZJU–UoE) Institute, Zhejiang University School of Medicine, Hangzhou 310058, Zhejiang, China

***Correspondence:** Bin Ma, School of Biomedical Engineering Med-X Research Institute, Shanghai Jiao Tong University, No. 3 Teaching Building, 1954 Huashan RD, Xuhui District, Shanghai 200030, China. binma@sjtu.edu.cn

Academic Editor: Fathia Mami-Chouaib, Université Paris-Saclay, France

Received: March 13, 2022 **Accepted:** October 29, 2022 **Published:** December 27, 2022

Cite this article: Yuan P, Zhou Y, Wang Z, Gui L, Ma B. Dendritic cell-targeting chemokines inhibit colorectal cancer progression. *Explor Target Antitumor Ther.* 2022;3:828–40. <https://doi.org/10.37349/etat.2022.00115>

Abstract

Aim: Recent progress in cancer immunotherapy has shown its promise and prompted researchers to develop novel therapeutic strategies. Dendritic cells (DCs) are professional antigen-presenting cells crucial for initiating adaptive anti-tumor immunity, therefore a promising target for cancer treatment. Here, anti-tumor activities of DC-targeting chemokines were explored in murine colorectal tumor models.

Methods: The correlation of chemokine messenger RNA (mRNA) expression with DC markers was analyzed using The Cancer Genome Atlas (TCGA) dataset. Murine colorectal tumor cell lines (CT26 and MC38) stably overexpressing mouse C-C motif chemokine ligand 3 (CCL3), CCL19, CCL21, and X-C motif chemokine ligand 1 (XCL1) were established by lentiviral transduction. The effect of chemokines on tumor cell proliferation/survival was evaluated *in vitro* by cell counting kit-8 (CCK-8) assay and colony formation assay. Syngeneic subcutaneous tumor models were used to study the effects of these chemokines on tumor growth. Ki-67 expression in tumors was examined by immunohistochemistry. Immune cells in the tumor microenvironment (TME) and lymph nodes were analyzed by flow cytometry.

Results: Expression of the four chemokines was positively correlated with the two DC markers [integrin alpha X (*ITGAX*) and *CLEC9A*] in human colorectal tumor samples. Tumoral overexpression of DC-targeting chemokines had little or no effect on tumor cell proliferation/survival *in vitro* while significantly suppressing tumor growth *in vivo*. Fluorescence-activated cell sorting (FACS) analysis showed that CCL19, CCL21, and XCL1 boosted the ratios of DCs and T cells in CD45⁺ leukocytes while CCL3 increased the percentage of CD45⁺ leukocytes in total cells in MC38 tumor. XCL1 had an additional positive effect on antigen uptake by DCs in the TME and antigen transfer to tumor-draining lymph nodes.

Conclusions: CCL3, CCL19, CCL21, and XCL1 exhibited potent anti-tumor activities *in vivo*, although they might differentially regulate immune cells in the TME and antigen transfer to lymph nodes.

Keywords

Dendritic cells, chemokines, tumor microenvironment, immunotherapy, colorectal cancer

© The Author(s) 2022. This is an Open Access article licensed under a Creative Commons Attribution 4.0 International License (<https://creativecommons.org/licenses/by/4.0/>), which permits unrestricted use, sharing, adaptation, distribution and reproduction in any medium or format, for any purpose, even commercially, as long as you give appropriate credit to the original author(s) and the source, provide a link to the Creative Commons license, and indicate if changes were made.



Introduction

Colorectal cancer (CRC) is the third most frequently occurring cancer and the second leading cause of cancer death worldwide in 2020 [1]. Despite the rapid development of checkpoint inhibition immunotherapy, it is only effective in a small proportion of CRC patients [2, 3]. Therefore, more immunotherapeutic strategies need to be explored for improved clinical outcomes.

The tumor microenvironment (TME) is one of the primary regulators of CRC development, metastasis, and resistance to therapies [4, 5]. CRC tumors evade immunosurveillance through various extrinsic mechanisms, including repression and exclusion of anti-tumor effector cells such as CD8⁺ T cells and dendritic cells (DCs), and accumulation of immunosuppressive cells in the TME such as regulatory T (Treg) cells and myeloid-derived suppressor cells (MDSCs) [6, 7]. DCs are crucial for inducing adaptive anti-tumor immune responses, especially the tumor-infiltrating conventional DCs (cDCs) [8–11]. Type 1 cDC (cDC1) is regarded as the main subset that can cross-present antigens to activate CD8⁺ T cells through the major histocompatibility complex (MHC)-I pathway, prime CD4⁺ T cells via MHC-II and CD40 signaling, and promote T helper 1 (Th1) and natural killer (NK) cells responses through interleukin (IL)-12 [8–10, 12, 13]. On the other hand, cDC2 can activate Th1, Th2, Th17, and CD8⁺ T cells *in vitro* and drive anti-tumor CD4⁺ T cell immunity [11, 14, 15]. Notably, cDCs are indispensable for adoptive T cell immunotherapy [16]. Therefore, efforts to increase cDCs in the TME would serve as an alternative therapeutic strategy and improve other immunotherapies' efficacies.

CD11c, encoded by the gene integrin alpha X (*ITGAX*), is a widely established marker for DCs. It is often employed to define DCs and their subsets [17, 18], and can be used as a prognostic marker for cancer and other diseases [19]. Human CD141⁺ DCs belong to cDC1, and are considered as the equivalents of the mouse CD8 α ⁺/CD103⁺ cDCs in functions and lineage [20]. And it is reported that human CD141⁺ DCs and mouse CD8 α ⁺/CD103⁺ cDCs both express C-type lectin receptor (CLR) CLEC9A which recognizes F-actin exposed by dead cells to mediate the cross-presentation process [21, 22]. CLEC9A has been used as a successful target for antibody-mediated delivery of antigens to cDC1 [23]. Overall, *ITGAX* and CLEC9A are favorable DC markers for total DC and cDC1 respectively for the analysis of patient samples consisting of various cell types.

Chemokines are important mediators of DC migration and play a significant role in coordinating anti-tumor immunity [24]. Various chemokines have abilities to recruit cDCs, including C-C motif chemokine ligand 3 (CCL3), CCL4, CCL5, CCL19, CCL20, CCL21, and X-C motif chemokine ligand 1 (XCL1) [25, 26]. Although upregulation of these chemokines in the TME is expected to enhance DC-mediated anti-tumor immunity, they may also exert pro-tumor behavior via regulation of tumor cells and other resident cells in the TME such as fibroblasts, endothelial cells, or other pro-tumorigenic immune cells [27–30]. While more evidence supports a pro-tumor role of CCL4, CCL5, and CCL20 [27–30], the effect of others may be context-dependent, indicating the complexity of the underlying interrelated signaling cascades [31, 32]. Therefore, CCL3, CCL19, CCL21, and XCL1 were eventually chosen as the focus of the current study. Despite a few reports suggesting that they participated in pro-tumor activities [31–33], we should not ignore their positive roles in eliciting anti-tumor immunity. In this study, we sought to determine whether those four chemokines could control tumor growth and regulate immune cells in murine models of CRC.

Materials and methods

Analysis of human The Cancer Genome Atlas database

The correlation of messenger RNA (mRNA) expression between chemokines and DC markers was analyzed using the cBioPortal (<http://www.cbioportal.org/>). Colorectal adenocarcinoma dataset of 592 samples with mRNA data (RNA Seq V2) from The Cancer Genome Atlas (TCGA), Pan-Cancer Atlas, was used for the analysis. Expression Z-scores of tumor samples compared to the expression distribution of all log-transformed mRNA expression of adjacent normal samples in the cohort (log RNA Seq V2 RSEM). The Z-score threshold was set at ± 2.0 . Analytical methods included both Spearman's rank correlation and Pearson correlation were calculated, and their correlation coefficients and respective *P* values were shown in the [Results](#).

Cell lines

CT26 and MC38 cell lines were cultured in Roswell Park Memorial Institute Medium (RPMI 1640) and Dulbecco's Modified Eagle Medium (DMEM), respectively, supplemented with 10% fetal bovine serum (FBS, Sigma-Aldrich) and 100 U/mL penicillin/streptomycin (Beyotime). Cell lines were authenticated by Shanghai Biowing Applied Biotechnology, and routinely tested for mycoplasma contamination. All cells were maintained in a 5% CO₂, humidified incubator at 37°C. CT26 and MC38 were infected with CCL3-, CCL19-, CCL21-, and XCL1-overexpressing lentiviruses co-expressing ZsGreen, in the presence of 6 µg/mL polybrene to generate cell lines stably expressing the chemokines or empty vector.

RNA extraction and quantitative reverse transcription-polymerase chain reaction

Total RNA was isolated by the RNA extraction kit (TIANGEN Biotech), and complementary DNA (cDNA) was synthesized by reverse transcription kit (Vazyme). Real-time polymerase chain reaction (PCR) was carried out using TB Green® *Premix Ex Taq*TM (Takara®) in the ABI 7900HT fast real-time PCR system (Applied Biosystems). mRNA expression levels of target genes were normalized to the glyceraldehyde 3-phosphate dehydrogenase (*Gapdh*) using the 2^{-ΔΔCt} method.

Cell counting kit-8 assay

Proliferation/survival of CT26 and MC38 cells overexpressing chemokines or vector was determined by cell counting kit-8 (CKK-8, TargetMol®) and measured by a microplate reader (Tecan Infinite® M Plex) every 24 h according to the protocols from the manufacturer.

Colony formation assay

Cells were plated at densities of 500, 1,000, and 2,000 cells/well in 12-well plates using a two-layer soft agar setting. The bottom of each well was covered by an agar layer, consisting of 1× DMEM complete medium with 0.6% (w/v) agarose. Subsequently, different concentrations of cells suspended in 1× DMEM complete medium with 0.35% (w/v) agarose were added on top of the bottom agar layer. After 10 days, colonies were stained with 0.005% crystal violet solution and counted using ImageJ software.

Syngeneic mouse models of CRC

Six- to eight-week-old male C57BL/6 mice and male BALB/c mice were purchased from Shanghai Lingchang BioTech Co., Ltd. The 0.5 × 10⁶ CT26 or 1 × 10⁶ MC38 cells overexpressing chemokines or vector were injected subcutaneously at the lower flank of mice in 100 µL phosphate-buffered saline (PBS) respectively. Tumor size was measured by a vernier caliper every three days and calculated as Tumor Volume (mm³) = Length (mm) × Width (mm) × Width (mm)/2. Mice were euthanized when tumor size reached 2,000 mm³ in volume or the tumor became ulcerated.

Immunohistochemistry

Whole tumors were fixed for 24 h in 4% formalin and subsequently embedded into paraffin, sectioned, and then mounted onto slides. After antigen retrieval, permeabilization, and blocking, anti-Ki-67 antibody (Abcam, ab16667) was incubated with the epitope at 4°C overnight, followed by the addition of horseradish peroxidase (HRP)-conjugated goat anti-rabbit immunoglobulin G (IgG; Abcam, ab6721, at 1:200 dilution) for another 30 min in dark at room temperature. Next, sections were treated with 3,3'-diaminobenzidine (DAB) substrate (Abcam, ab64238) and imaged by microscope (Leica DM6 B). The ratio of Ki-67⁺ cells was analyzed using ImageJ software. Four different fields were counted to calculate the average ratio for each tumor.

Flow cytometry

Mice were euthanized via CO₂ asphyxiation 15 days after the establishment of MC38 tumors. Tumor tissues were excised and cut into 1–2 mm³ pieces, and then treated with 1 mg/mL LiberaseTM TL (Roche) and 100 mg/mL DNase I (Sigma-Aldrich) in gentleMACSTM Octo Dissociator (Miltenyi Biotec). After dissociation of tumor tissues, cell suspensions were passed through 70-µm cell strainers (BioFil®) and washed twice with

PBS containing 2% FBS. Inguinal lymph nodes were mechanically dissociated and passed through 70- μ m cell strainers (BioFil®) to obtain single-cell suspensions.

Before antibody staining, single-cell suspensions were stained with Zombie dyes (BioLegend®) at a dilution of 1:200 for 10 min at room temperature to exclude dead cells. Markers on the cell surface were detected by staining cells with fluorochrome-labeled antibodies in PBS containing 2% FBS and 1 mmol/L ethylenediaminetetraacetic acid (EDTA) for 30 min on ice. For subsequent intracellular cytokine analysis, cells were washed once with PBS and treated with the True-Nuclear™ Transcription Factor Buffer Set (BioLegend®). The following antibodies were used: CD45 (30-F11, BD Biosciences, dilution 1:200); CD11c (N418, BioLegend®, dilution 1:100); CD11b (M1/70, BioLegend®, dilution 1:100); CD103 (2E7, BioLegend®, dilution 1:100); Ly6C (HK1.4, BioLegend®, dilution 1:100); CD64 (X54-5/7.1, BioLegend®, dilution 1:100); MHC-II (I-A/I-E, M5/114.15.2, BioLegend®, dilution 1:100); CD3e (145-2C11, BioLegend®, dilution 1:100); CD4 (GK1.5, BioLegend®, dilution 1:100); NK1.1 (PK136, BioLegend®, dilution 1:100); CD8a (53-6.7, BioLegend®, dilution 1:100); Foxp3 (MF-14, eBioscience, dilution 1:100). The cDCs were defined as: CD45⁺CD11c⁺MHC-II⁺CD64⁻Ly6C⁻; the cDC1: CD45⁺CD11c⁺MHC-II⁺CD64⁻Ly6C⁻CD103⁺; the cDC2: CD45⁺CD11c⁺MHC-II⁺CD64⁻Ly6C⁻CD11b⁺; the macrophages: CD11b⁺CD64⁺Ly6C⁻; the conventional CD4⁺ T cells: CD45⁺CD3e⁺CD4⁺Foxp3⁻; the Treg cells: CD45⁺CD3e⁺CD4⁺Foxp3⁺; the CD8⁺ T cells: CD45⁺CD3e⁺CD8⁺; the NK cells: CD45⁺CD3e⁻NK1.1⁺; the NKT cells: CD45⁺CD3e⁺NK1.1⁺. Fluorescence data were acquired on a BD LSRFortessa™ cell analyzer (BD Biosciences). Data were analyzed on FlowJo™ software.

Statistical analysis

Statistical tests were performed in GraphPad Prism 8. CCK-8 assay, colony formation assay, immunohistochemistry, and tumor growth *in vivo* were analyzed via two-way analysis of variance (ANOVA) followed by multiple comparisons; data from flow cytometry were analyzed via one-way ANOVA followed by multiple comparisons. Results were presented as mean values \pm standard error of the measurement (SEM), and $P < 0.05$ was considered statistically significant.

Results

Expression of *CCL3*, *CCL19*, *CCL21*, and *XCL1* correlates with DC markers in human CRC patient samples

To explore the potential *in vivo* role of the selected chemokines in regulating DCs in human CRC patients, we first analyzed the correlation of their mRNA expression with DC markers. Expression of all the four chemokine genes, including *CCL3*, *CCL19*, *CCL21*, and *XCL1*, was positively correlated with that of both *ITGAX* encoding the general DC marker CD11c and *CLEC9A*, which is a cDC1 marker, in human CRC samples (Figure 1) [34]. These findings implied that all the four chemokines played a positive role in DC infiltration in human colorectal tumors, although they might have discrepant activities in regulating different DC subsets and other immune cells.

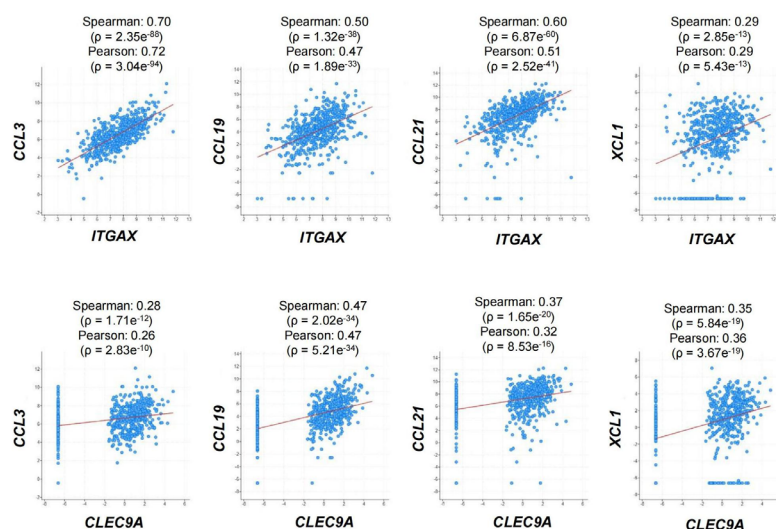


Figure 1. Correlation of mRNA expression between chemokines and DC markers. RNA-sequencing dataset from 592 colorectal adenocarcinoma patients (TCGA, Pan-Cancer Atlas) was used to analyze the expression correlation between *CCL3/CCL19/CCL21/XCL1* and *ITGAX/CLEC9A*. Dot plots indicate mRNA expression levels in tumor samples relative to normal samples (Z-score, log₂ RNA Seq V2 RSEM)

Tumoral overexpression of DC-targeting chemokines showed no or little effects on tumor cell proliferation/survival *in vitro*

To clarify the anti- or pro-tumor effects of the DC-targeting chemokines, we generated murine CRC cell lines that stably expressed the four chemokines. Successful overexpression of mouse *CCL3*, *CCL19*, *CCL21*, and *XCL1* (encoded by *Ccl3/Ccl19/Ccl21/Xcl1*) in CT26 and MC38 cell lines was confirmed by quantitative reverse transcription-PCR (Figure 2A and 2B). CCK-8 assay demonstrated that overexpression of these genes did not significantly change the total numbers of cells during the 72-h culture period, compared to empty vector control, except that *CCL3* and *CCL21* reduced the growth rate of CT26 cells but to a limited extent (Figure 2C and 2D). Moreover, the colony-forming ability of MC38 cells was not affected by these chemokines (Figure 2E). It suggested that the chemokines had trivial or no direct effect on the proliferation or survival of tumor cells.

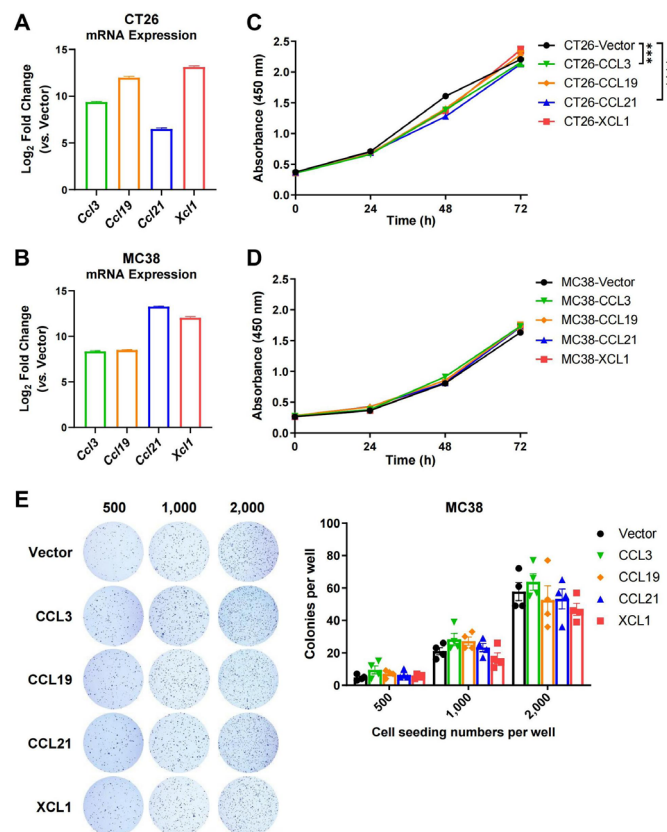


Figure 2. Chemokine overexpression hardly affects tumor cell proliferation or survival. A. and B. The expression of mouse chemokine genes (*Ccl3/Ccl19/Ccl21/Xcl1*) in CT26 (A) and MC38 (B) cell lines was confirmed by quantitative PCR (qPCR, $n = 4-5$); C. and D. CCK-8 assay was used to quantify the amount of CT26 (C, $n = 3$) and MC38 cells (D, $n = 5$) overexpressing chemokines or vector over a 72-h culture period; E. representative images for colony formation assay and statistics of colony numbers of MC38 overexpressing chemokines or empty vector at indicated seeding densities ($n = 4$). *** $P < 0.001$; **** $P < 0.0001$

Tumoral overexpression of DC-targeting chemokines inhibits tumor growth in mice

We then established subcutaneous tumor models using CT26 and MC38 overexpressing the four chemokines. In both models, tumoral overexpression of *CCL3*, *CCL19*, *CCL21*, and *XCL1* significantly repressed tumor growth (Figure 3A-C), despite the differential overexpression levels in these cell lines (Figure 2A and 2B). Consistently, these chemokines also decreased the ratio of Ki-67⁺ cells in MC38 tumors indicating a negative effect on tumor cell growth *in vivo* (Figure 4A and 4B). Taking the results from CT26 and MC38 models together, *CCL19* seemed to be the most potent anti-tumor chemokine among the four. Since these chemokines

had no or little effects on the proliferation or survival of tumor cells (Figure 2C and 2D), their anti-tumor activities *in vivo* were very likely to depend on their immunomodulatory effects in the TME.

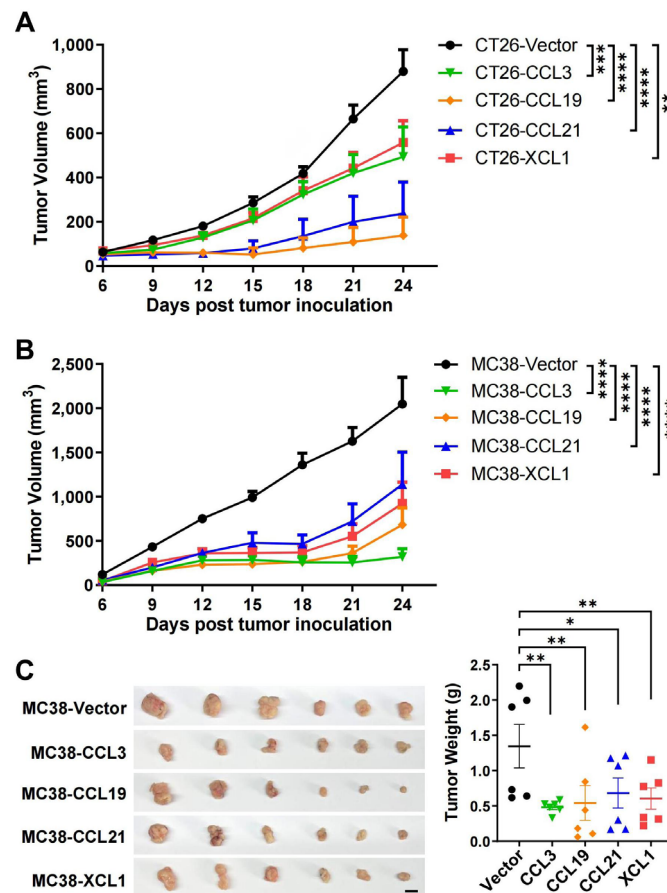


Figure 3. Tumoral overexpression of chemokines inhibits colorectal tumor growth. Volumes of CT26 tumors ($n = 5/\text{group}$, A) or MC38 tumors ($n = 8/\text{group}$, B) overexpressing chemokines or vector were monitored overtime; C. images and weights of MC38 tumors, scale bar = 1 cm. * $P < 0.05$; ** $P < 0.01$; *** $P < 0.001$; **** $P < 0.0001$

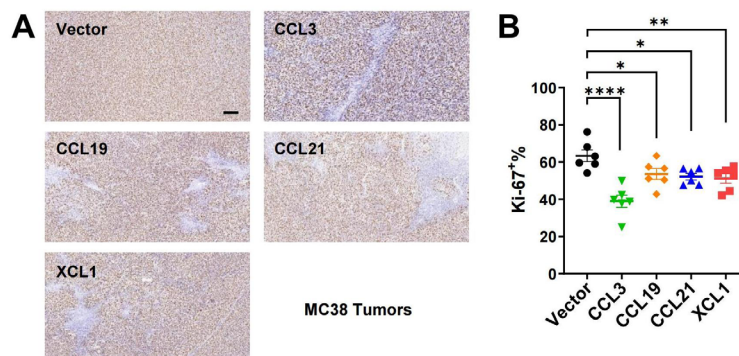


Figure 4. Immunohistochemistry for Ki-67 in MC38 tumors. A. Representative images of Ki-67 staining, scale bar = 50 μm ; B. statistics of Ki-67⁺ ratios ($n = 6/\text{group}$). * $P < 0.05$; ** $P < 0.01$; **** $P < 0.0001$

Regulation of DCs in MC38 tumors and lymph nodes by chemokines

Next, we sought to investigate the effects of these chemokines on DC migration in MC38 tumor models by fluorescence-activated cell sorting (FACS). MC38 cells expressed ZsGreen simultaneously as an indicator of tumor-specific antigen. Tumoral overexpression of CCL19, CCL21, and XCL1 significantly increased ratios of total cDCs, cDC1, and cDC2 subtypes among CD45⁺ leukocytes in the TME, as compared to the empty vector control tumors (Figure 5A and 5B). However, CCL3 did not change the ratios of total cDCs or the two subtypes. In contrast, the percentages of macrophages were not affected by either chemokine, suggesting these chemokines were DC-specific. In particular, the ratio of ZsGreen⁺ cDCs was upregulated in XCL1-overexpressing tumors, suggesting an enhanced uptake of tumor antigens (Figure 5C).

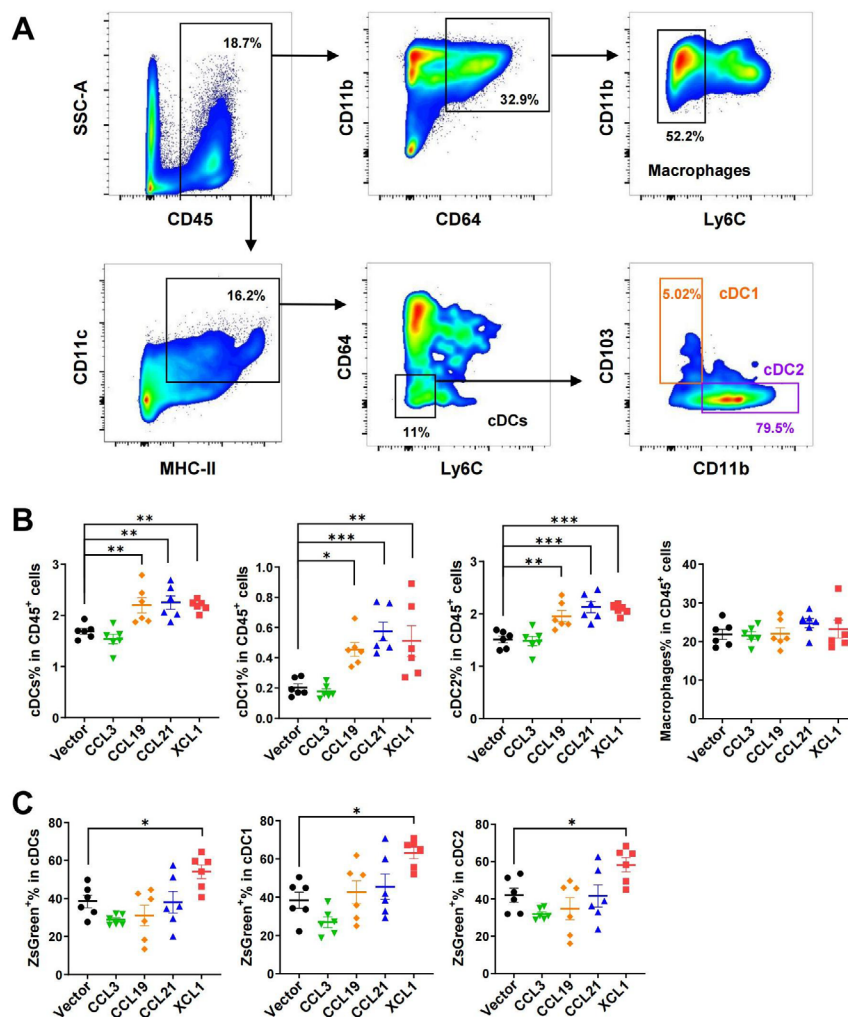


Figure 5. FACS analysis of tumor-infiltrating cDCs and macrophages in MC38 tumor model. A. Gating strategies for cDCs, cDC1, cDC2, and macrophages; B. ratios of cDCs, cDC1, cDC2, and macrophages in CD45⁺ cells; C. ratios of ZsGreen⁺ cells in cDCs. * $P < 0.05$; ** $P < 0.01$; *** $P < 0.001$; SSC-A: side scatter-area

Interestingly, cDCs, including cDC1 and cDC2 in the tumor-draining lymph nodes, were significantly decreased by tumoral expression of these chemokines, implying an efflux of cDCs from the lymph nodes or a biased upregulation of other immune cells such as T cells upon antigen presentation and stimulation (Figure 6A and 6B). Higher percentages of ZsGreen⁺ cDCs were found in the lymph nodes of CCL3- and XCL1-overexpressing tumor models (Figure 6C). This finding suggested that more tumor antigens were delivered by cDCs from tumors overexpressing these two chemokines, and possibly more tumor-specific T cells would be generated. The increased tumor antigen ZsGreen in the lymph nodes of XCL1-overexpressing tumor models may be partially attributed to the increased antigen uptake in the tumor (Figure 5C). These data demonstrated that tumoral expression of these chemokines did not impair or even promote the antigen transfer from the tumor site to tumor-draining lymph nodes.

Regulation of tumor-infiltrating lymphocytes by chemokines

Confirming a positive effect on cDCs in TME and lymph nodes, we further analyzed the tumor-infiltrating effector lymphocytes by FACS (Figure 7A). CD45⁺ leukocytes in total live cells were upregulated only in CCL3-overexpressing tumors, although the ratios of lymphocytes in CD45⁺ cells were not changed by CCL3 (Figure 7B). Consistent with their effects on cDCs, CCL19, CCL21, and XCL1 significantly increased the ratios of conventional Foxp3⁺CD4⁺ T and CD8⁺ T cells. These three chemokines also elevated ratios of Treg cells, although the effect of CCL19 was not statistically significant. NK cells were upregulated by CCL19 and XCL1, while CCL19, CCL21, and XCL1 upregulated NKT. Together, these results revealed that these chemokines boosted anti-tumor adaptive immunity and enrichment of other effector cells with anti-tumor activities such as NK and NKT cells.

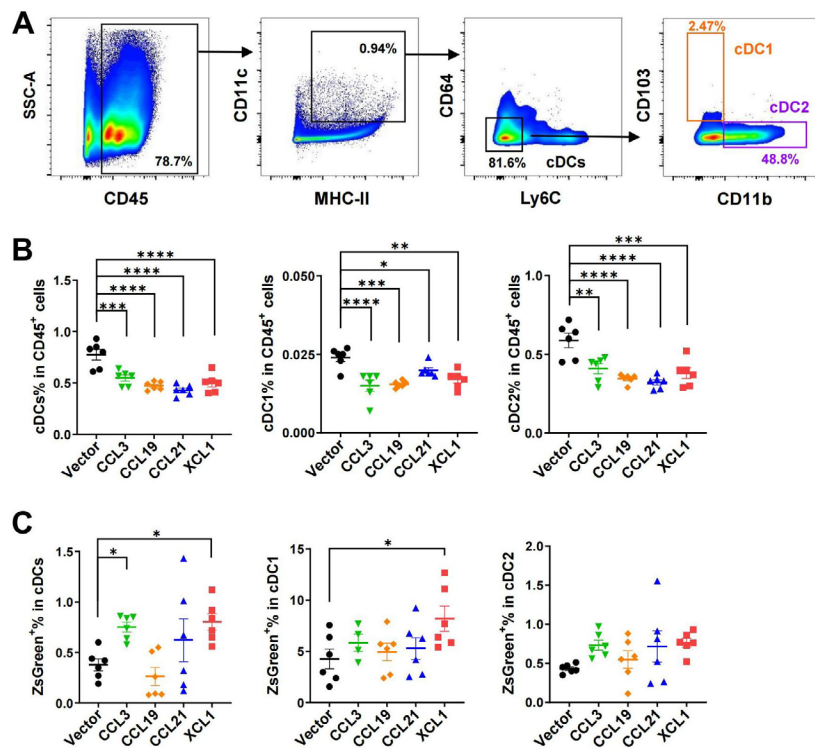


Figure 6. FACS analysis of cDCs in tumor-draining lymph nodes in MC38 tumor model. A. Gating strategies for cDCs, cDC1, and cDC2; B. ratios of cDCs, cDC1, and cDC2 in CD45⁺ cells; C. ratios of ZsGreen⁺ cells in cDCs. * $P < 0.05$; ** $P < 0.01$; *** $P < 0.001$; **** $P < 0.0001$

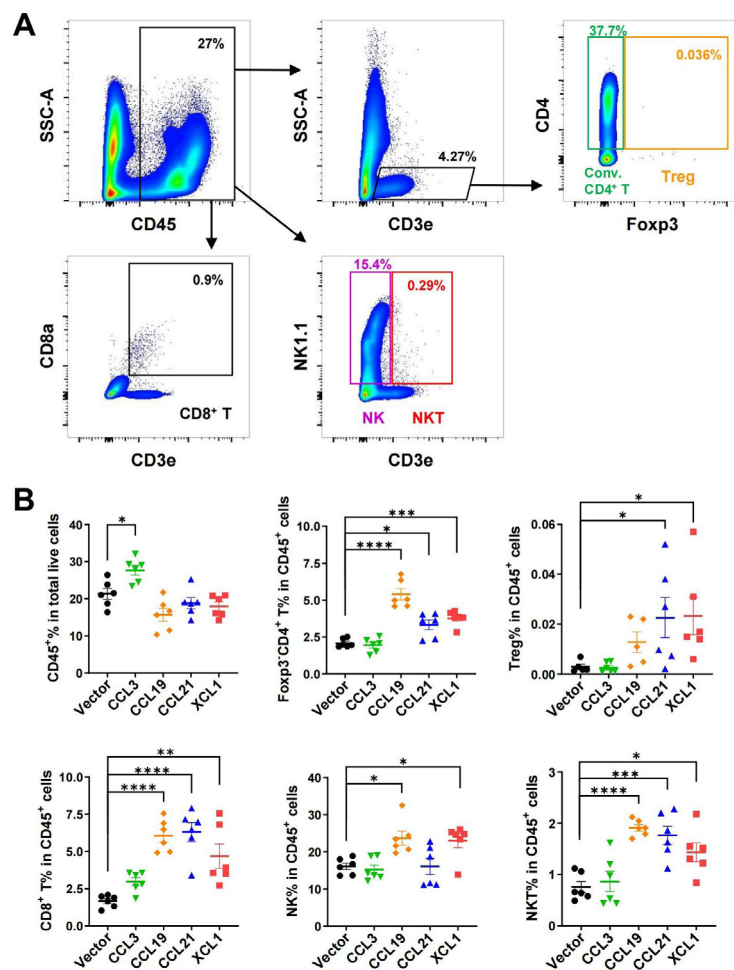


Figure 7. FACS analysis of tumor-infiltrating lymphocytes in MC38 tumor model. A. Gating strategies for conventional (conv.) CD4⁺ T, Treg, CD8⁺ T, NK, and NKT cells; B. ratio of CD45⁺ cell in total live cells, and ratios of lymphocytes in CD45⁺ cells. * $P < 0.05$; ** $P < 0.01$; *** $P < 0.001$; **** $P < 0.0001$

Discussion

In agreement with their anti-tumor potentials, a higher density of tumor-infiltrating cDCs is associated with a better prognosis for patients with various tumor types [35–37]. Here we evaluated the anti-tumor activities of several DC-targeting chemokines in parallel to explore the possibility of using them for immunotherapy. We focused on the chemokines with less evidence of a pro-tumor role. In mouse CRC models, we demonstrated that all four chemokines, including CCL3, CCL19, CCL21, and XCL1, effectively inhibited tumor growth. Since these chemokines showed hardly any effect on the proliferation/survival of tumor cells *in vitro*, their functions *in vivo* would largely depend on the regulation of TME cells. Accordingly, they significantly increased the ratios of cDCs and T cells in CD45⁺ cells in the MC38 tumor, except CCL3 (Figures 5 and 7). However, CCL3 was the only chemokine that upregulated the percentage of CD45⁺ cells out of total cells from the tumor (Figure 7B), suggesting it might have a broad impact on a variety of leukocytes leading to an unbiased ratio of cDCs or T cells in CD45⁺ cells. Indeed, CCL3 has a complex role in mediating a great range of cell types via three distinct receptors, including C-C motif chemokine receptor 1 (CCR1), CCR4, and CCR5 [25, 38]. Interestingly, our FACS analysis indicated that CCL3 promoted the transfer of tumor antigens to lymph nodes (Figure 6C). As a result, it can be speculated that more tumor-specific T cells will appear, contributing to the anti-tumor activity of CCL3.

Both CCL19 and CCL21 signal through CCR7 and are essential to building an effective interaction between T cells and DCs in lymphoid tissues [25, 38]. Differing from CCL19, CCL21 has a long C-terminal tail with 37 amino acids and is competent to interact with glycosaminoglycans (GAGs) and then immobilizes the chemokine [39, 40], which may explain the differential activities of these two chemokines [41]. CCL21 was shown to be superior to CCL19 in promoting chimeric antigen receptor (CAR)-T activity [41]. In both CT26 and MC38 tumor models of our study, CCL19 and CCL21 showed powerful anti-tumor activities, with CCL19 being more potent than CCL21 (Figure 3), although the overexpression levels varied in the two tumor cell lines. In addition to a role in recruiting cDCs, CCL19 and CCL21 may also induce the proinflammatory differentiation program in DCs [42]. Moreover, they may regulate migration and proliferation/survival of T cells [43, 44]. The other mechanisms besides DC recruitment added to the complexity of their anti-tumor actions. Accordingly, in MC38 tumors, conventional CD4⁺ T and CD8⁺ T cells were boosted by these two chemokines. Notably, CCL19 overexpression induced higher ratios of tumor-infiltrating conventional CD4⁺ T and NK cells but fewer Treg cells compared to CCL21, which may partially contribute to the more prominent anti-tumor effect of CCL19. Nevertheless, both seem to be promising immunotherapeutic molecules, and more context-dependent studies are needed to select the optimal one.

Consistent with the previous report that XCL1 was able to attract CD103⁺ DCs in murine models [45, 46], XCL1 was found to increase CD103⁺ cDC1 and CD11b⁺ cDC2 in MC38 tumors in our study (Figure 5B). Furthermore, our findings also revealed an unexpected role of XCL1 in enhancing tumor antigen uptake by cDCs and antigen transfer to lymph nodes (Figure 5C and 6C). Whether the regulation of DC function by XCL1 is via direct activation of X-C motif chemokine receptor 1 (XCR1) on DCs remains to be elucidated.

The major limitation of the current study is that the overexpression levels of these chemokines were not equal in tumor cells due to technical difficulties. Thus, the study of these chemokines by tumoral overexpression is relatively qualitative, and a comparison of their activities is somewhat preliminary and suggestive. However, CCL19 seemed to be the most potent anti-tumor chemokine among the four if considering results from both CT26 and MC38 models. Nevertheless, our study still provides the foundation for prompting these chemokines into more sophisticated preclinical studies.

A variety of DC-based immunotherapeutic strategies are being perused in preclinical and clinical studies [34]. The delivery of DC-targeting chemokines to the tumor site represents an ideal way to boost local anti-tumor immunity. This approach may stand alone or be combined with other immunotherapies such as immune checkpoint inhibition. Recent progress in tumor-targeting nanoparticles [47], and cellular vehicles such as mesenchymal stem cells [48, 49], will facilitate more precise delivery of these chemokines to the tumor site to generate the chemotactic gradients and local effects.

Abbreviations

CCK-8: cell counting kit-8
CCL3: C-C motif chemokine ligand 3
CCR1: C-C motif chemokine receptor 1
cDC1: type 1 conventional dendritic cell
cDCs: conventional dendritic cells
CRC: colorectal cancer
DCs: dendritic cells
DMEM: Dulbecco's Modified Eagle Medium
FACS: fluorescence-activated cell sorting
FBS: fetal bovine serum
ITGAX: integrin alpha X
MHC: major histocompatibility complex
mRNA: messenger RNA
NK: natural killer
PBS: phosphate-buffered saline
PCR: polymerase chain reaction
Th1: T helper 1
TME: tumor microenvironment
Treg: regulatory T
XCL1: X-C motif chemokine ligand 1

Declarations

Author contributions

PY, YZ, ZW, and LG: Data curation, Validation. BM: Conceptualization, Supervision. PY and BM: Formal analysis, Writing—original draft, Writing—review & editing. All listed authors read and approved the final manuscript.

Conflicts of interest

The authors declare that they have no conflicts of interest.

Ethical approval

All animal procedures were approved by the Institutional Animal Care and Use Committee (IACUC) and the Bioethics Committee of School of Biomedical Engineering, Shanghai Jiao Tong University, Shanghai, China.

Consent to participate

Not applicable.

Consent to publication

Not applicable.

Availability of data and materials

Not applicable.

Funding

This work was supported by funds from Science and Technology Commission of Shanghai Municipality [20ZR1426500 to BM]. The funder had no role in study design, data collection and analysis, decision to publish, or preparation of the manuscript.

References

1. Sung H, Ferlay J, Siegel RL, Laversanne M, Soerjomataram I, Jemal A, et al. Global cancer statistics 2020: GLOBOCAN estimates of incidence and mortality worldwide for 36 cancers in 185 countries. *CA Cancer J Clin*. 2021;71:209–49.
2. Ooki A, Shinozaki E, Yamaguchi K. Immunotherapy in colorectal cancer: current and future strategies. *J Anus Rectum Colon*. 2021;5:11–24.
3. Morad G, Helmink BA, Sharma P, Wargo JA. Hallmarks of response, resistance, and toxicity to immune checkpoint blockade. *Cell*. 2021;184:5309–37.
4. Quail DF, Joyce JA. Microenvironmental regulation of tumor progression and metastasis. *Nat Med*. 2013;19:1423–37.
5. Tauriello DVF, Calon A, Lonardo E, Batlle E. Determinants of metastatic competency in colorectal cancer. *Mol Oncol*. 2017;11:97–119.
6. Koi M, Carethers JM. The colorectal cancer immune microenvironment and approach to immunotherapies. *Future Oncol*. 2017;13:1633–47.
7. Legitimo A, Consolini R, Failli A, Orsini G, Spisni R. Dendritic cell defects in the colorectal cancer. *Hum Vaccin Immunother*. 2014;10:3224–35.
8. Ferris ST, Durai V, Wu R, Theisen DJ, Ward JP, Bern MD, et al. cDC1 prime and are licensed by CD4⁺ T cells to induce anti-tumour immunity. *Nature*. 2020;584:624–9.
9. Roberts EW, Broz ML, Binnewies M, Headley MB, Nelson AE, Wolf DM, et al. Critical role for CD103⁺/CD141⁺ dendritic cells bearing CCR7 for tumor antigen trafficking and priming of T cell immunity in melanoma. *Cancer Cell*. 2016;30:324–36.
10. Salmon H, Idoyaga J, Rahman A, Leboeuf M, Remark R, Jordan S, et al. Expansion and activation of CD103⁺ dendritic cell progenitors at the tumor site enhances tumor responses to therapeutic PD-L1 and BRAF inhibition. *Immunity*. 2016;44:924–38.
11. Binnewies M, Mujal AM, Pollack JL, Combes AJ, Hardison EA, Barry KC, et al. Unleashing type-2 dendritic cells to drive protective antitumor CD4⁺ T cell immunity. *Cell*. 2019;177:556–71.e16.
12. Haniffa M, Shin A, Bigley V, McGovern N, Teo P, See P, et al. Human tissues contain CD141^{hi} cross-presenting dendritic cells with functional homology to mouse CD103⁺ nonlymphoid dendritic cells. *Immunity*. 2012;37:60–73.
13. Poulin LF, Salio M, Griessinger E, Anjos-Afonso F, Craciun L, Chen JL, et al. Characterization of human DNGR-1⁺ BDCA3⁺ leukocytes as putative equivalents of mouse CD8α⁺ dendritic cells. *J Exp Med*. 2010;207:1261–71.
14. Nizzoli G, Larghi P, Paroni M, Crosti MC, Moro M, Neddermann P, et al. IL-10 promotes homeostatic proliferation of human CD8⁺ memory T cells and, when produced by CD1c⁺ DCs, shapes naive CD8⁺ T-cell priming. *Eur J Immunol*. 2016;46:1622–32.
15. Di Blasio S, Wortel IMN, van Bladel DAG, de Vries LE, Duiveman-de Boer T, Worah K, et al. Human CD1c⁺ DCs are critical cellular mediators of immune responses induced by immunogenic cell death. *Oncoimmunology*. 2016;5:e1192739.
16. Spranger S, Dai D, Horton B, Gajewski TF. Tumor-residing Batf3 dendritic cells are required for effector T cell trafficking and adoptive T cell therapy. *Cancer Cell*. 2017;31:711–23.e4.
17. Balan S, Saxena M, Bhardwaj N. Chapter one - dendritic cell subsets and locations. *Int Rev Cell Mol Biol*. 2019;348:1–68.

18. Wu J, Wu H, An J, Ballantyne CM, Cyster JG. Critical role of integrin CD11c in splenic dendritic cell capture of missing-self CD47 cells to induce adaptive immunity. *Proc Natl Acad Sci U S A*. 2018;115:6786–91.
19. Wang Y, Xu B, Hu WW, Chen LJ, Wu CP, Lu BF, et al. High expression of CD11c indicates favorable prognosis in patients with gastric cancer. *World J Gastroenterol*. 2015;21:9403–12.
20. Radford KJ, Tullett KM, Lahoud MH. Dendritic cells and cancer immunotherapy. *Curr Opin Immunol*. 2014;27:26–32.
21. Sancho D, Joffre OP, Keller AM, Rogers NC, Martínez D, Hernanz-Falcon P, et al. Identification of a dendritic cell receptor that couples sensing of necrosis to immunity. *Nature*. 2009;458:899–903.
22. Zhang JG, Czabotar PE, Policheni AN, Caminschi I, Wan SS, Kitsoulis S, et al. The dendritic cell receptor Clec9A binds damaged cells via exposed actin filaments. *Immunity*. 2012;36:646–57.
23. Tullett KM, Leal Rojas IM, Minoda Y, Tan PS, Zhang JG, Smith C, et al. Targeting CLEC9A delivers antigen to human CD141⁺ DC for CD4⁺ and CD8⁺T cell recognition. *JCI Insight*. 2016;1:e87102.
24. Gunn MD, Kyuwa S, Tam C, Kakiuchi T, Matsuzawa A, Williams LT, et al. Mice lacking expression of secondary lymphoid organ chemokine have defects in lymphocyte homing and dendritic cell localization. *J Exp Med*. 1999;189:451–60.
25. Nagarsheth N, Wicha MS, Zou W. Chemokines in the cancer microenvironment and their relevance in cancer immunotherapy. *Nat Rev Immunol*. 2017;17:559–72.
26. Viola A, Sarukhan A, Bronte V, Molon B. The pros and cons of chemokines in tumor immunology. *Trends Immunol*. 2012;33:496–504.
27. Mukaida N, Sasaki SI, Baba T. CCL4 signaling in the tumor microenvironment. In: Birbrair A, editor. *Tumor microenvironment*. Cham: Springer International Publishing; 2020. pp. 23–32.
28. Aldinucci D, Borghese C, Casagrande N. The CCL5/CCR5 axis in cancer progression. *Cancers (Basel)*. 2020;12:1765.
29. Kadomoto S, Izumi K, Mizokami A. The CCL20-CCR6 axis in cancer progression. *Int J Mol Sci*. 2020;21:5186.
30. Chen W, Qin Y, Liu S. CCL20 signaling in the tumor microenvironment. In: Birbrair A, editor. *Tumor microenvironment*. Cham: Springer International Publishing; 2020. pp. 53–65.
31. Ntanasis-Stathopoulos I, Fotiou D, Terpos E. CCL3 signaling in the tumor microenvironment. In: Birbrair A, editor. *Tumor microenvironment*. Cham: Springer International Publishing; 2020. pp. 13–21.
32. Gowhari Shabgah A, Jaber Al-Obaidi ZM, Rahman HS, Abdelbasset WK, Suksatan W, Bokov DO, et al. Does CCL19 act as a double-edged sword in cancer development? *Clin Exp Immunol*. 2021;207:164–75.
33. Korbecki J, Grochans S, Gutowska I, Barczak K, Baranowska-Bosiacka I. CC chemokines in a tumor: a review of pro-cancer and anti-cancer properties of receptors CCR5, CCR6, CCR7, CCR8, CCR9, and CCR10 ligands. *Int J Mol Sci*. 2020;21:7619.
34. Wculek SK, Cueto FJ, Mujal AM, Melero I, Krummel MF, Sancho D. Dendritic cells in cancer immunology and immunotherapy. *Nat Rev Immunol*. 2020;20:7–24.
35. Kashimura S, Saze Z, Terashima M, Soeta N, Ohtani S, Osuka F, et al. CD83⁺ dendritic cells and Foxp3⁺ regulatory T cells in primary lesions and regional lymph nodes are inversely correlated with prognosis of gastric cancer. *Gastric Cancer*. 2012;15:144–53.
36. Xiao Y, Li H, Mao L, Yang QC, Fu LQ, Wu CC, et al. CD103⁺ T and dendritic cells indicate a favorable prognosis in oral cancer. *J Dent Res*. 2019;98:1480–7.
37. Szpor J, Streb J, Glajcar A, Fraczek P, Winiarska A, Tyrak KE, et al. Dendritic cells are associated with prognosis and survival in breast cancer. *Diagnostics (Basel)*. 2021;11:702.
38. Schaller TH, Batich KA, Suryadevara CM, Desai R, Sampson JH. Chemokines as adjuvants for immunotherapy: implications for immune activation with CCL3. *Expert Rev Clin Immunol*. 2017;13:1049–60.
39. Yan Y, Chen R, Wang X, Hu K, Huang L, Lu M, et al. CCL19 and CCR7 expression, signaling pathways, and adjuvant functions in viral infection and prevention. *Front Cell Dev Biol*. 2019;7:212.

40. Jørgensen AS, Rosenkilde MM, Hjortø GM. Biased signaling of G protein-coupled receptors - from a chemokine receptor CCR7 perspective. *Gen Comp Endocrinol*. 2018;258:4–14.
41. Luo H, Su J, Sun R, Sun Y, Wang Y, Dong Y, et al. Coexpression of IL7 and CCL21 increases efficacy of CAR-T cells in solid tumors without requiring preconditioned lymphodepletion. *Clin Cancer Res*. 2020;26:5494–505.
42. Marsland BJ, Bättig P, Bauer M, Ruedl C, Lässig U, Beerli RR, et al. CCL19 and CCL21 induce a potent proinflammatory differentiation program in licensed dendritic cells. *Immunity*. 2005;22:493–505.
43. Flanagan K, Moroziewicz D, Kwak H, Horig H, Kaufman HL. The lymphoid chemokine CCL21 costimulates naive T cell expansion and Th1 polarization of non-regulatory CD4⁺ T cells. *Cell Immunol*. 2004;231:75–84.
44. Förster R, Davalos-Misslitz AC, Rot A. CCR7 and its ligands: balancing immunity and tolerance. *Nat Rev Immunol*. 2008;8:362–71.
45. Dorner BG, Dorner MB, Zhou X, Opitz C, Mora A, Guttler S, et al. Selective expression of the chemokine receptor XCR1 on cross-presenting dendritic cells determines cooperation with CD8⁺ T cells. *Immunity*. 2009;31:823–33.
46. Crozat K, Guiton R, Contreras V, Feuillet V, Dutertre CA, Ventre E, et al. The XC chemokine receptor 1 is a conserved selective marker of mammalian cells homologous to mouse CD8α⁺ dendritic cells. *J Exp Med*. 2010;207:1283–92.
47. Swain S, Sahu PK, Beg S, Babu SM. Nanoparticles for cancer targeting: current and future directions. *Curr Drug Deliv*. 2016;13:1290–302.
48. Chulpanova DS, Kitaeva KV, Tazetdinova LG, James V, Rizvanov AA, Solovyeva VV. Application of mesenchymal stem cells for therapeutic agent delivery in anti-tumor treatment. *Front Pharmacol*. 2018;9:259.
49. Yin P, Gui L, Wang C, Yan J, Liu M, Ji L, et al. Targeted delivery of CXCL9 and OX40L by mesenchymal stem cells elicits potent antitumor immunity. *Mol Ther*. 2020;28:2553–63.